Si(111)7×7 and Si(111)$\sqrt{3}\times\sqrt{3}$-Al surface-structure analysis by ion-induced Auger-electron spectroscopy

T. Aizawa,* T. Tsuno, H. Daimon, and S. Ino
Department of Physics, Faculty of Science, University of Tokyo, 7-3-1 Hongo, Bunkyo-ku, Tokyo 113, Japan
(Received 27 May 1987)

Si(111)7×7 and Si(111)$\sqrt{3}\times\sqrt{3}$-Al surface structures have been studied by ion-induced Auger-electron spectroscopy. It has been revealed that the azimuthal dependence of the Auger-electron yield is very sensitive to differences in surface atomic structure at grazing ion incidence. Experimental results have been compared with computer simulations. It has been found that the dimer-adatom stacking-fault model is best as the Si(111)7×7 structure model, and as yet no model proposed for the Si(111)$\sqrt{3}\times\sqrt{3}$-Al structure has been satisfactory.

INTRODUCTION

Ion-induced Auger-electron spectroscopy (IAES) has been used for surface analysis since Musket and Bauer[1] showed its merits. Recently, Schuster and Varelas[2,3] showed that IAES is a powerful technique for surface-atomic-structure analysis when combined with surface ion channeling. They applied the technique to the Ni(110)-O system and analyzed the atomic configuration.

Ion-scattering spectroscopy (ISS) is usually used for surface-atomic-structure analysis. The advantages of IAES compared with ISS are thought to be the following.

(1) When a light ion is used as a projectile, the excitation process is considered to be simple, and complicated charge-exchange processes such as ion neutralization or reionization can be neglected.

(2) It is easy to resolve two elements with similar mass numbers. For example, although very high angular and energy resolution are required to distinguish Al from Si in an ISS experiment, such a distinction is easy in an IAES experiment.

(3) Both Si and Al have very high excitation cross sections, so the IAES has a very high degree of sensitivity to such elements.

In this paper, Si(111)7×7, Si(111)$\sqrt{3}\times\sqrt{3}$-Al, and Si(111)$\sqrt{7}\times\sqrt{7}$-Al structures are investigated by the IAES technique. These structures have been subject to a lot of investigation. Very recently, several probable models were proposed for the clean Si(111)7×7 structure.[4–11] For Al-covered Si(111) surfaces, Lander and Morrison[12] discovered several phases by low-energy electron diffraction (LEED) investigation more than 20 years ago. Of these phases, a Si(111)$\sqrt{3}\times\sqrt{3}$-Al structure at $\frac{1}{3}$-ML Al coverage (ML denotes monolayer) is thought to be easier to analyze than any other semiconductor-metal system, because the unit cell of this structure is relatively small and contains only one adsorbate atom in it. Recently Northrup[13] calculated the total energy and the surface electronic band structures of two adsorption models of this Si(111)$\sqrt{3}\times\sqrt{3}$-Al structure. One is the so-called T_4 model, in which the Al adsorbate atom sits on a threefold hollow site above the second-layer Si atom. The other is the H_3 model, in which Al sits on the other threefold hollow site. Northrup has concluded that the T_4 model is better than the H_3 model because the former has lower total energy when displacements of substrate atoms are allowed. Some angle-resolved ultraviolet photoemission spectroscopy (ARUPS) studies[14,15] and an inverse photoemission study[16] of this surface have been done and their results agree very well with the band structure calculated by Northrup, but the band dispersion relations of these two models resemble each other. The difference in the absolute value of the surface-state energies between the H_3 model and the T_4 model is not so large. It is yet to be determined which model shall most likely be correct.

EXPERIMENTAL PROCEDURES

An apparatus was newly constructed in our laboratory. As is schematically shown in Fig. 1, it consists of a UHV scattering chamber, a differentially pumped ion gun, a cylindrical mirror analyzer (CMA), a reflection high-energy electron diffraction (RHEED) system, a two-axis rotatable manipulator, and some evaporators. The scattering chamber is made of SUS-304 stainless

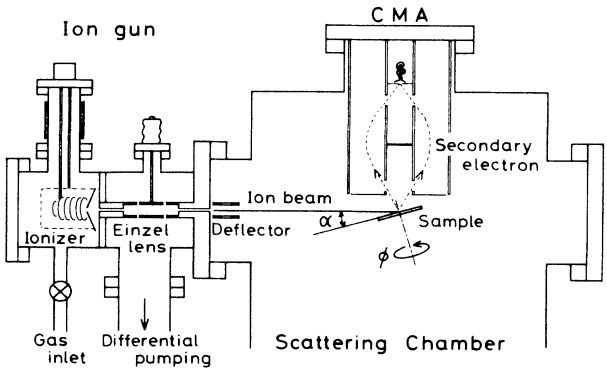

FIG. 1. Schematic view of the apparatus. α is the glancing angle of incidence to the surface plane and ϕ the azimuthal angle of incidence.

steel and can be baked up to 200 °C. Its diameter is 400 mm and the height is about 1000 mm. It was pumped by a 500-l/s sputter ion pump, and after 12 h baking the base pressure was less than 5×10^{-10} torr. The ion gun consists of a B-A gauge-type electron-impact ionization cell, a pair of collimators that have 3-mm diameter and 40-mm length, an electrostatic lens between them, and an x-y deflector. The lens chamber between the ionization cell and the scattering chamber was differentially pumped by a 300-l/s turbo molecular pump, so that total pressure in the scattering chamber was kept at less than 1×10^{-9} torr even when gas was introduced into the ionization cell in the order of 10^{-5} torr. This ion gun produces a beam of which the diameter is about 3 mm and the divergence is less than 0.01 rad at an ion beam energy of 24 keV. The beam current was about 5 nA at the sample position. Our apparatus does not contain any mass separating system, so when H_2 gas is used as an ion source, H^+ ions may come out as well as H_2^+ ions. Under our conditions it is assured, from the energy spectrum of ions scattered by the sample, that the number of H^+ ions in the primary beam is less than $\frac{1}{10}$ that of the H_2^+ ions.

When a sample is irradiated with the ion beam, secondary electrons, including Auger electrons, are emitted. These are detected by the CMA, which is placed just above the sample as shown in Fig. 1. The energy resolution of the CMA is a few eV, and that value is enough to resolve the Auger signals into each other. In Fig. 2 a typical secondary electron energy spectrum is shown. At 86 and 64 eV, *LVV* or *LMM* Auger peaks of Si and Al are seen, respectively. Si Auger intensity was determined by subtracting the secondary electron yield at the high-energy-side foot (point *B* in Fig. 2) from the yield at the peak position (point *A*). Al intensity was determined in the same way. It has been reported that the ion-induced Si Auger peak has the complicated structure.[17] Namely, the peak consists of the so-called atomiclike peak at 86 eV and the bulklike shoulder at 91 eV.

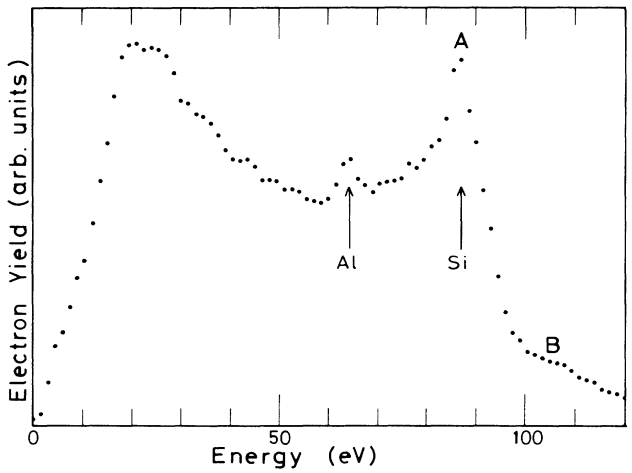

FIG. 2. Typical secondary electron energy spectrum induced by 24-keV H_2^+-ion beam. The sample is Si(111)$\sqrt{7}\times\sqrt{7}$-Al (coverage is about 1 ML); $\alpha=15°$; ϕ is random.

The cause of these structures is thought to be the difference in positions where excited recoiling target atoms emit the Auger electrons. Here these two were not resolved because the important point is not where the target atoms emit electrons but where they have been excited.

In this experiment we have measured the Auger intensity dependence on the ion incident azimuth. As the ion gun is fixed, the ion incident azimuth was changed by rotating the sample around an axis perpendicular to the sample surface. If the emitted Auger electron has some angular distribution for the crystal orientation, the detected Auger intensity may be affected by this angular distribution while the sample is rotated. But, it has been confirmed that the effect is very small, because the CMA has fairly wide angular acceptance range. Actually the Auger intensity scarcely changed during the azimuth rotation under the present experimental condition with the electron-induced AES.

Samples consisted of a mirror-polished Si(111) surface, in which the deviation from (111) was less than 1°. A commercially produced boron-doped p-type single crystal with a resistivity of 18–25 Ω cm was used. The crystal thickness is about 0.45 mm. The crystal was cut by cleavage into a rectangular form (4×25 mm^2) and was fitted on a sample holder made of Ta. The sample was cleaned by resistive heating up to 1250 °C in a 10^{-10}-torr order vacuum for a few minutes. Then RHEED showed a clear 7×7 reconstructed pattern.[18] When about $\frac{1}{3}$-ML Al was adsorbed with the sample maintained at a temperature of 660 °C, the surface structure changed completely to $\sqrt{3}\times\sqrt{3}(R\pm30°)$. This was called α-$\sqrt{3}\times\sqrt{3}$ structure by Lander and Morrison.[12] The $\sqrt{7}\times\sqrt{7}(R\pm19.1°)$ structure was formed when more than $\frac{2}{3}$-ML Al was applied at 550 °C.[14] These three reconstructed surfaces were investigated in this work.

EXPERIMENTAL RESULTS

Figure 3 shows the dependences of Si *LVV* Auger intensity on the incident azimuth of the ion beam measured for the 7×7, the $\sqrt{3}\times\sqrt{3}$, and the $\sqrt{7}\times\sqrt{7}$ structures. Considering the threefold symmetry and the existence of the mirror planes, the azimuthal scanning range was taken from $[2\bar{1}\bar{1}]$ ($\phi=-30°$) to $[11\bar{2}]$ ($\phi=+30°$). The energy of the incident H_2^+ ion beam was 24 keV and its glancing angle α was 15°. At this α, surface channeling does not occur, so these three data have very similar shapes. Though we can see some differences in detail, it is considered to be difficult at this level of experimental accuracy to obtain the information about surface structures from such minor differences between the data. On the contrary, as is shown in Fig. 4, the Si Auger yield is seen to be very sensitive to the surface structure when the ion incident angle is set to a grazing angle ($\alpha=2.0\pm0.5°$), where surface channelings can occur.

In Fig. 4(a) the datum of the clean 7×7 structure is shown. It has one deep dip at the $[10\bar{1}]$ azimuth ($\phi=0°$) whose full width at the half depth is about 5°, and there are peaks at both sides of the dip ($\phi=\pm7°$) and a shoulderlike structure can be seen between the maximum of

the peak and the minimum of the dip. There are dips at $[2\bar{1}\bar{1}]$ ($\phi=-30°$) and $[11\bar{2}]$ ($\phi=30°$) directions whose widths are about 3°, and around them very small dips exist at $\phi=\pm25°$. Broad and shallow dips are seen around $\phi=\pm15°$. In Fig. 5(a) the truncated bulk structure is shown. As is seen in Fig. 5(b), the first dip ($\phi=0°$) is correlated with the channeling direction in which the nearest-neighbor atoms exist, and the second two ($\phi=\pm30°$) are the second nearest ones. The direction in which the third nearest atom exists is the same as the first one and the fourth ones are at $\phi=\pm19°$. But in the experimental datum no dip can be seen in the directions of $\phi=\pm19°$.

Figure 4(b) is the datum for the Si(111)$\sqrt{3}\times\sqrt{3}$-Al surface structure. There are dips also at $\phi=0°$ and $\phi=\pm30°$, and new dips can be seen at $\phi=\pm11°$ and $\phi=\pm16°$. The dips at $\phi=\pm30°$ are wider (the width is about 8°) and deeper than those of the 7×7 structure. These directions are the nearest neighbors of the $\sqrt{3}\times\sqrt{3}$ unit cell [Fig. 5(d)]. The dip at $\phi=0°$ has almost the same width as that of the 7×7 structure although the dip in the 7×7 surface has the extra structures mentioned above. The directions $\phi=\pm11°$ are the fourth nearest directions, and $\phi=\pm16°$ are the seventh nearest directions. The azimuthal dependence of the Al Auger intensity is almost similar to that of Si except that the dips at $\phi=\pm30°$ are a little wider than those of Si.

In the case of the $\sqrt{7}\times\sqrt{7}$-Al structure, as is shown in Fig. 4(c), the dip profile is different from that of the 7×7 structure and that of the $\sqrt{3}\times\sqrt{3}$ structure. It also has dips at $\phi=\pm30°$, but in this case the dip has a complex structure. At $\phi=-21°$ and $-18°$ dips partially overlap each other. At $\phi=18°$ and 21° there are the same complex dips. Dips are also seen at $\phi=\pm11°$ and very small dips occur at $\phi=\pm5°$. In the two-domain $\sqrt{7}\times\sqrt{7}$ structure, the essential directions are $\phi=\pm19.1°$. But in the datum, the dip around this direction is divided into two dips. As this datum is thought

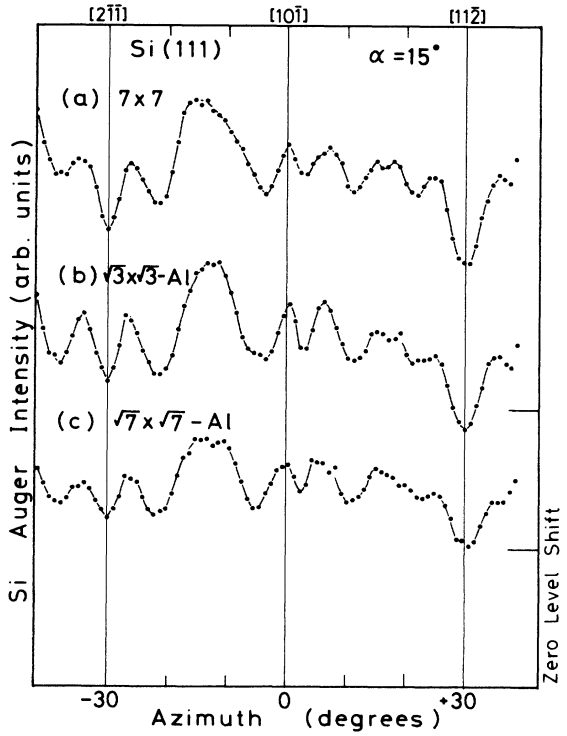

FIG. 3. Experimental data of the Si *LVV* Auger-electron intensity dependence on the ion incident azimuth. $\alpha=15°$. Primary H_2^+-ion beam energy is 24 keV. The lines are intended to be a guide for the eyes. (a) Si(111)7×7 clean surface, (b) Si(111)$\sqrt{3}\times\sqrt{3}$-Al reconstructed surface, and (c) Si(111)$\sqrt{7}\times\sqrt{7}$-Al reconstructed surface.

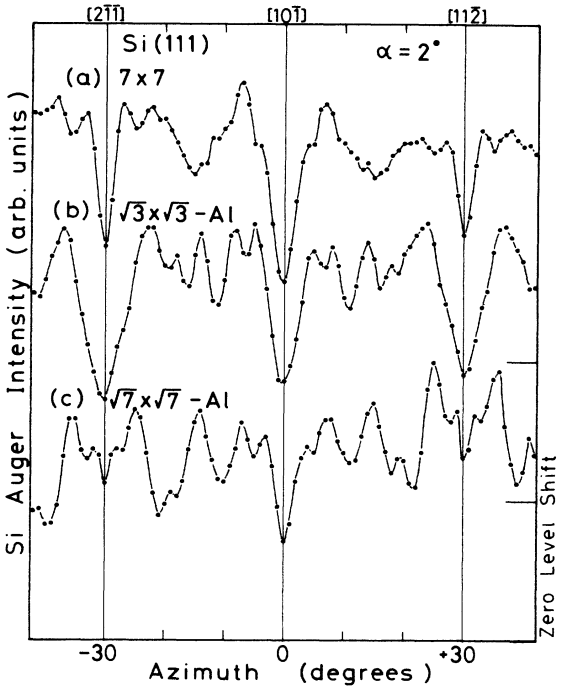

FIG. 4. Experimental data of the Si *LVV* Auger-electron yield dependence on the ion incident azimuth. $\alpha=2°$. The lines are only intended to be a guide for the eyes. Ion energy is 24 keV. Samples are the same as Fig. 3.

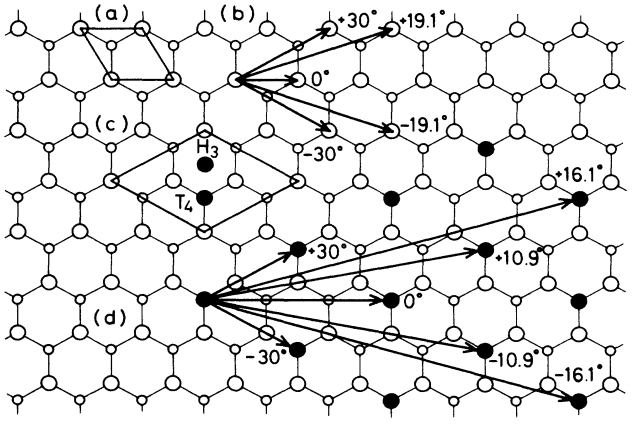

FIG. 5. (a) Unit cell of nonreconstructed Si(111) surface. (b) Azimuthal directions of near atoms on Si(111)1×1. (c) Unit cell of $\sqrt{3}\times\sqrt{3}$ surface. H_3 and T_4 are the adsorption sites mentioned in the text. (d) Azimuthal directions of near adsorbates on the Si(111)$\sqrt{3}\times\sqrt{3}$ reconstructed surface.

to be very difficult to interpret, we have not tried to analyze it in this paper.

COMPUTER SIMULATION

Monte Carlo simulations for several models of the 7×7 and the $\sqrt{3}\times\sqrt{3}$ structures were carried out to analyze the data. The method of the simulation is similar to that of Schuster and Varelas.[3] The trajectories of ions are calculated one by one and the calculations start when the incident ion arrives at a height of 1.5 Å above the outermost atomic layer. Thus the initial z position is fixed. The initial x-y position is assumed to be uniformly distributed over the unit cell. The initial kinetic energy and the initial glancing angle are fixed. More than 1000 trajectories were calculated for one azimuthal angle.

One ion goes straight, except that it is scattered by other atoms. Considering interactions with electrons in the crystal, the ion loses kinetic energy at a finite rate (assumed here to be 10 eV/Å). This calculation takes into account only a binary collision. Namely, only when the projectile passes with an impact parameter of less than 1.0 Å, it is regarded to be scattered. The scattering angle is calculated approximating the potential between the ion and the atom as a Thomas-Fermi-Molière potential.[19] The probability of making a vacancy in the core level of the target atom is simultaneously evaluated according to the table of Hansteen *et al.*[20] In this case, the ionization process is regarded to be a Coulomb ionization. The probability is accumulated in each azimuth and each target atom. The direction of motion and the kinetic energy of the ion are changed according to the scattering geometry. The trajectory starts once more from the scattering position. When the projectile goes out of the unit cell, it is returned back into the same unit cell. One trajectory calculation is stopped and the next starts when the ion leaves the surface, or when it goes deeply into the bulk, or when the kinetic energy of the ion becomes so small (less than 5 keV) that the excitation probability is negligible. Thus the ionization probabilities of each target atom are accumulated, and they are summed up taking into account the escape length of the Auger electrons.

In this calculation, thermal vibrations and steps are taken into account. The lattice vibrational effect is considered by moving atoms randomly around their equilibrium positions. The displacement of the atom from its equilibrium position is assumed to have a Gaussian-type distribution with the width of a bulk root-mean-square vibrational amplitude [0.078 Å at 50 °C, corresponding to the Debye temperature of 543 K (Ref. 21)]. The effect of the steps is taken into account by transferring the projectile at a finite rate according to the step density along the vector that indicates a step height and a lateral shift of the unit cell between the upper side and the lower side of the step. Here a mean terrace length of a few hundred angstroms was used. It was reported by Schuster and Varelas[22] that this surface channeling method was very sensitive to steps when the incident ion beam energy was higher and the glancing angle was lower. But with the energy and the glancing angle used here, our simulations show that the existence of steps slightly increases the base intensity of Auger electrons and hardly changes the profile of dips or peaks.

RESULTS AND DISCUSSION

Inasmuch as the energy of the incident H_2^+ ion is high (24 keV), we assume that the molecular form is of no consequence. Therefore, a H^+ ion with a half energy of 12 keV is used in the simulation. The computer simulations were carried out for six different models of the 7×7 structure and for several models of the $\sqrt{3}\times\sqrt{3}$ structure. For the 7×7 models, Tromp and van Loenen[23] showed that models which contain stacking faults reproduced their experimental results from medium-energy ion scattering (MEIS) very well. They rejected all models which do not contain stacking faults, because the simulations could not reproduce their experimental data. Comparing their computer simulations and also taking into consideration transmission electron diffraction (TED) data, they concluded that the relaxed McRae's model and Takayanagi's model were the best of the remaining stacking-fault models. So we have chosen for our simulations mainly the models containing stacking faults. For instance, McRae's stacking-fault model,[4] Himpsel and Batra's trimer model,[5] Bennett's stacking-fault and adatom model,[6] and Takayanagi *et al.*'s

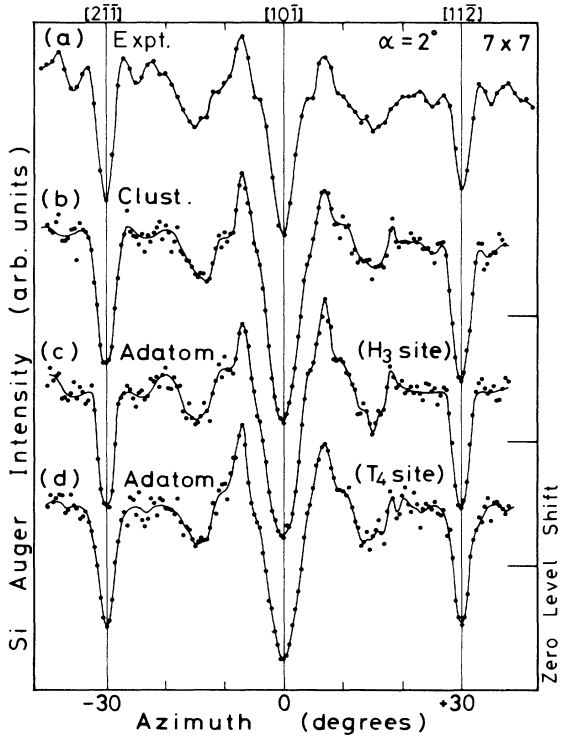

FIG. 6. Dependence of the Si LVV Auger-electron yield on the ion incident azimuth. $\alpha=2°$. The lines are only intended to be a guide for the eyes. (a) Experimental result same as Fig. 4(a). The sample is a clean Si(111)7×7 reconstructed surface. (b), (c), and (d) are simulations for the pyramidal cluster model (Ref. 8), the H_3-site adatom model (Ref. 10), and the T_4-site adatom model, respectively.

dimer-adatom stacking-fault (DAS) model[7] were used. The pyramidal cluster model[8,9] and the adatom models[10] were also tried. The displacement model proposed by Ino *et al.*[11] is not tried in this paper because it is very difficult to evaluate the actual displacement values of each atom quantitatively.

Figures 6–8 show the IAES experimental data and simulation results of these models. Figure 6(b) is the simulation for the pyramidal cluster model.[8,9] Main dips ($\phi=0°,\pm30°$) and shallow dips ($\phi=\pm15°$) are reproduced. But the small dips at $\phi=\pm25°$ which are seen in Fig. 6(a) are not clearly seen in Fig. 6(b). The deepest dip at $\phi=0°$ does not have the shoulderlike structure and is a little wider than the experimental one. Figure 6(c) is the result for the adatom model proposed by Binnig.[10] Here the adatoms' height is assumed to be 1.1 Å above the first Si layer. Figure 6(d) is the result for the adatom model in which the 12 adatoms rest at T_4 sites instead of H_3 sites as in Binnig's model. Both models have the feature similar to that of the pyramidal cluster model except that the dip at $\phi=0°$ becomes asymmetric and wider. Agreement between each of these three models and the experiment is reasonable. Next, in Figs. 7(b), 7(c), and 7(d) the simulation results for Himpsel and Batra's model,[5] Bennett's model,[6] and McRae's model[4] are indicated, respectively. None of these models can reproduce the experimental data. On the contrary, Takayanagi's model[7] reproduces our data very well (Fig. 8). All dips and shoulderlike structures seen in the experimental data are reproduced in the simulation results. So it can be concluded that Takayanagi's model is the best of all proposals. As far as the authors know, this is the first experiment using an ion beam that is able to discriminate clearly among the models which contain stacking faults. In the model corresponding to Fig. 8(b), the dimer length is $\frac{2}{3}a$ ($a=3.84$ Å), the adatom height is 1.33 Å from the first layer, and the other atoms are not relaxed. In this model the dip shapes at $\phi=\pm15°$ (positions *B* and *C* in Fig. 8) are a little different from the observed one. And the small dips at $\phi=\pm25°$ (positions *A* and *D*) are not so clear. Figure 8(c) is the result for a relaxed DAS model that is calculated by Yamaguchi[24] with a Keating-type energy minimization method. In this case the dips at *B* and *C* deviate from the experimental data. Finally, Fig. 8(d) corresponds to another relaxed DAS model that is calculated by Qian and Chadi[25] using a total energy minimization method. This result agrees with the experimental data best of all. So it can be concluded that this model is the most reliable as the 7×7 reconstruction model at present.

From these results it can also be concluded that this

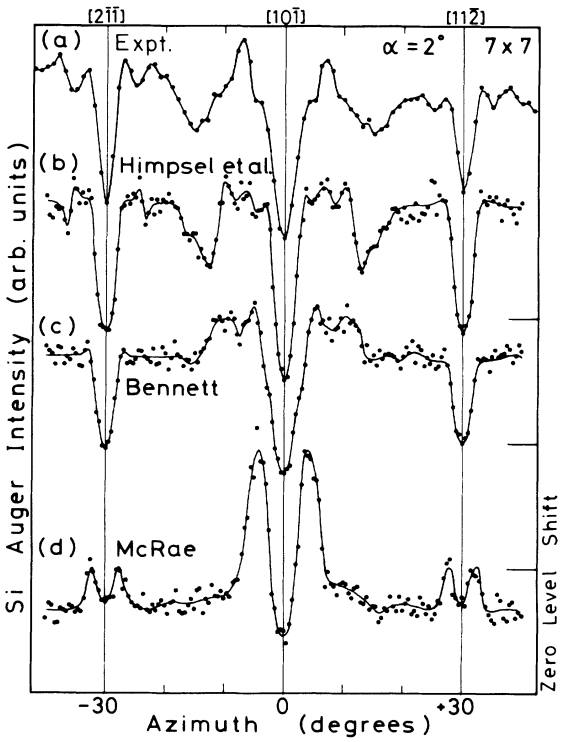

FIG. 7. Dependence of the Si *LVV* Auger-electron yield on the ion incident azimuth. $\alpha=2°$. The lines are only intended to be a guide for the eyes. (a) Experimental result same as Fig. 4(a). The sample is a clean Si(111)7×7 reconstructed surface. (b), (c), and (d) are simulations for Himpsel and Batra's stacking-fault trimer model,[5] Bennett's stacking-fault adatom model,[6] and McRae's stacking-fault model,[4] respectively.

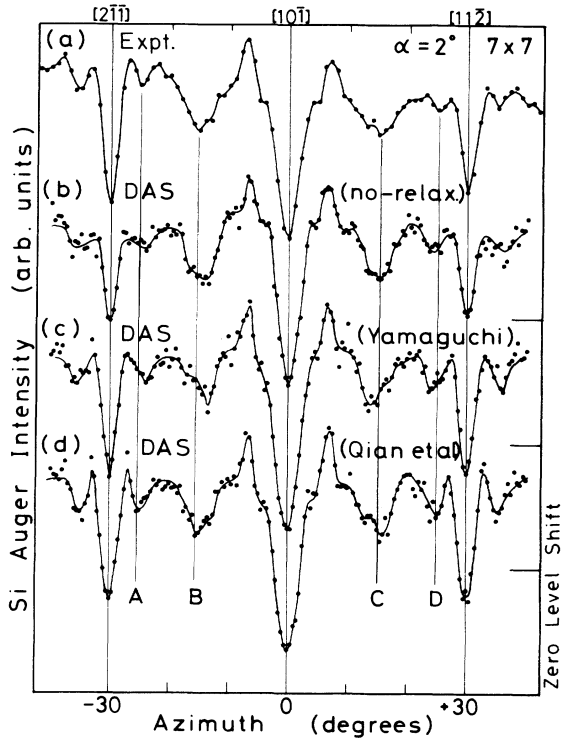

FIG. 8. Dependence of the Si *LVV* Auger-electron yield on the ion incident azimuth. $\alpha=2°$. The lines are only intended to be a guide for the eyes. (a) Experimental result same as Fig. 4(a). The sample is a clean Si(111)7×7 reconstructed surface. (b) Simulation for the unrelaxed DAS model (Ref. 7). The height of the adatoms is 1.33 Å. (c) Simulation for the relaxed DAS model calculated by Yamaguchi (Ref. 24). (d) Simulation for the relaxed DAS model calculated by Qian and Chadi (Ref. 25). Differences are seen on the dip positions and the dip shapes at *A*, *B*, *C*, and *D*.

IAES method is powerful enough not only to estimate rough atomic structures but also to analyze detailed atomic configurations such as lattice relaxations. But the simulations of the adatom models and the pyramidal cluster model yield similar results in spite of the different atomic configurations. A probable reason for this result is that the method is very sensitive to the lateral correlation of atoms which are positioned at comparable heights, and the sensitivity is high especially to the outermost atomic layer. For example, as McRae's model does not have adatoms, it gives a completely different result from others. The DAS model, the pyramidal cluster model, and the adatom models have the same outermost layer, so it is thought that these models produced similar results in the simulations.

For the $\sqrt{3}\times\sqrt{3}$ structure, the T_4-site adsorption model proposed by Northrup[13] (T_4), a nonrelaxed H_3-site adsorption model (H_3), a nonrelaxed on-top site adsorption model (OT), a substitution model for the first-layer Si atom (SB), and a pyramidal cluster $\sqrt{3}\times\sqrt{3}$ model (CL) were tested. The results are shown in Figs. 9–12. With respect to Si Auger data (Figs. 9 and 11), T_4, H_3, OT, and CL yield similar results. Al data (Figs. 10 and 12) are similar, too, except for a small difference seen in the H_3 result. This may be due to the similarity of the outermost Al atom configurations. Figures 11(c) and 12(c) correspond to the SB model, in which the Al atom is relaxed 0.2 Å outward. Figures 11(d) and 12(d) correspond to the similar model in which Al is relaxed inward. The following points can be seen comparing Fig. 12(c) with Fig. 12(d). When Al is the outermost [in the case of (c)], Al Auger intensity is varied largely and many dips are observable. On the contrary, when Al is lowered, dips can be seen only along the main directions. This indicates again that the IAES is mainly affected by the outermost layer, and subangstrom deviations in this layer are distinguishable by this method.

All models except the SB models show all dips observed in the experiment. But the minimum yields at the dips are much lower than those seen in the experimental data. Namely, in the simulations, the bottoms of the dips at $\phi=\pm 30°$ are almost zero. However, in the experiment, the bottom yields are at least $\frac{1}{2}-\frac{1}{3}$ of the mean yield. Because quick measurements are necessary, a simple method for the estimation of the Auger intensity has been used, so the absolute value of the experimental Auger yield may not be so accurate quantitatively. But in the 7×7 case we obtained satisfactory results. So it can be said that this disagreement is not due to experimental inaccuracy, but due to the incompleteness of the models. Moreover, the shapes of the dips at $\phi=\pm 30°$ are different. Specifically, the peaks at both sides of the dip are too large in the simulations of Si Auger intensities (Fig. 9). When the incident glancing angle α is too low, these peaks tend to become large and the bottom

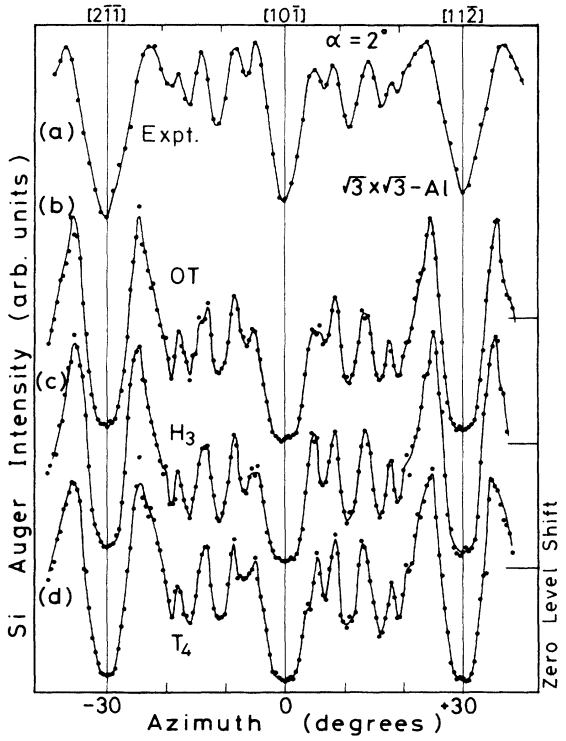

FIG. 9. Dependence of the Si LVV Auger-electron yield on the ion incident azimuth. $\alpha=2°$. The lines are only intended to be a guide for the eyes. (a) Experimental result. The sample is a Si(111)$\sqrt{3}\times\sqrt{3}$-Al reconstructed surface. (b) Simulation for the on-top site adsorption model. Adsorbate height is 2.4 Å above the first-layer Si. (c) Simulation for the H_3-site adsorption model. Adsorbate height is 1.1 Å. (d) Simulation for the relaxed version of the T_4-site adsorption model calculated by Northrup (Ref. 13).

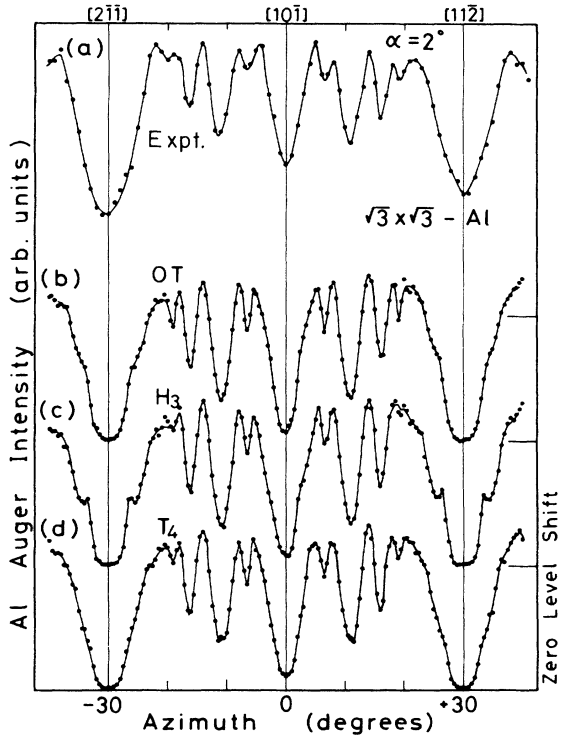

FIG. 10. Dependence of the Al LVV Auger-electron yield on the ion incident azimuth. $\alpha=2°$. The lines are only intended to be a guide for the eyes. The models are the same as in Fig. 9.

yield tends to become small. Although it is not shown here, when α is increased, these peaks become smaller and the minimum yield becomes larger. But simultaneously, Al Auger intensity simulations become completely different from the experimental one. So it can be concluded that any simple model is not satisfactory. Several other models were tried although they are not shown here. Any model in which Al height is near to the Si layer (for example, substitution to the second layer and relaxed outward model), or a model in which randomly oriented trimers are arranged to $\sqrt{3}\times\sqrt{3}$ structure, etc., cannot reproduce the experimental data at all. Perhaps we must construct a more complex model taking into account the domain size, multidomain structures, or randomness of the surface unit cell, for example, the nonunity probability of occupancy of one atomic site, etc.

In a related investigation, high-resolution electron energy loss spectroscopy (HREELS) was carried out on this structure and one vibrational mode of 65 meV was discovered.[26] But this mode was concluded not to be an adsorbate-substrate vibration mode because the same modes appeared both on Al-induced and In-induced $\sqrt{3}\times\sqrt{3}$ surfaces.[27] This may also be inconsistent with simple adsorption models such as T_4 or H_3.

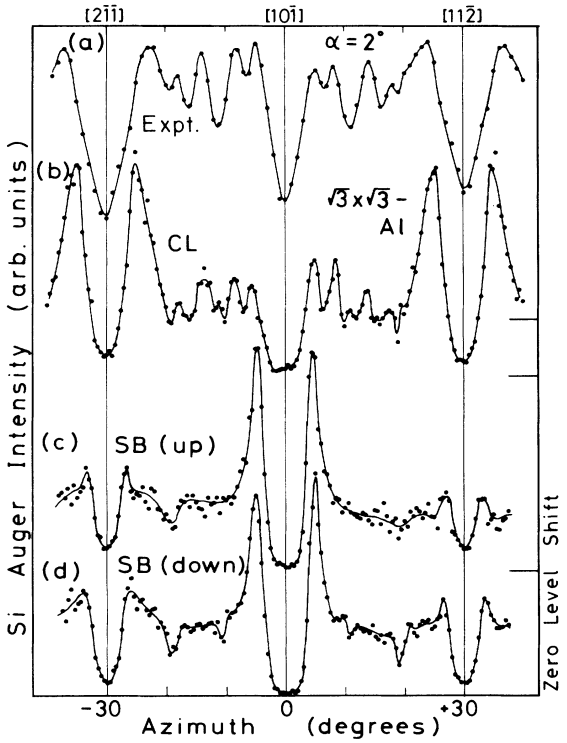

FIG. 11. Dependence of the Si *LVV* Auger-electron yield on the ion incident azimuth. $\alpha=2°$. The lines are only intended to be a guide for the eyes. (a) Experimental result. The sample is a Si(111)$\sqrt{3}\times\sqrt{3}$-Al reconstructed surface. (b) Simulation for the cluster model. (c) Simulation for the model in which Al substitutes for the first-layer Si and is relaxed 0.2 Å outward. (d) Simulation for the similar model to (c) in which Al is relaxed 0.2 Å inward.

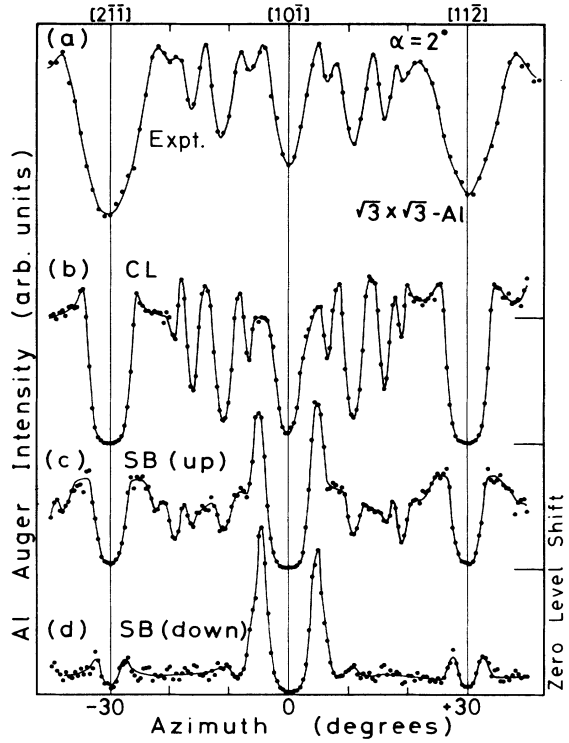

FIG. 12. Dependence of the Al *LVV* Auger-electron yield on the ion incident azimuth. $\alpha=2°$. The lines are only intended to be a guide for the eyes. The models are the same as in Fig. 11.

SUMMARY

A new apparatus was constructed for surface-structure analysis by the IAES method. It is indicated that when the ion incident angle is set to the grazing angle, this method is very sensitive to surface reconstructions, especially to the outermost atomic configurations. This method was applied to the Si(111) surface and we conclude that the DAS model is the best of all proposals for the Si(111)7×7 surface reconstruction, and that no model proposed thus far is satisfactory for the Si(111)$\sqrt{3}\times\sqrt{3}$-Al surface.

It was also shown that this method has a high sensitivity to the lattice relaxation in the vicinity of the surface, and that the relaxation of the DAS model calculated by Qian and Chadi is reliable. Although it is difficult to create a new surface reconstruction model from IAES data only, this method is very powerful in judging whether or not a proposed model is accurate.

ACKNOWLEDGMENTS

We would like to thank Dr. R. Souda for very stimulating discussions. The calculations were done on the FACOM M-340S system at the National Institute for Research in Inorganic Materials. The present work was supported in part by a Grant-in-aid for Special Distinguished Research Project (60065003) from the Ministry of Education, Science and Culture, and in part by Toray Science and Technology Grants of the Toray Science Foundation.

*Present address: National Institute for Research in Inorganic Materials, 1-1 Namiki, Sakura-mura, Niihari-gun, Ibaraki 305, Japan.

[1]R. G. Musket and W. Bauer, Thin Solid Films **19**, 69 (1973).
[2]M. Schuster and C. Varelas, Surf. Sci. **134**, 195 (1983).
[3]M. Schuster and C. Varelas, Nucl. Instrum. Methods B **9**, 145 (1985).
[4]E. G. McRae, Phys. Rev. B **28**, 2305 (1983).
[5]F. J. Himpsel and Inder P. Batra, J. Vac. Sci. Technol. A **2**, 952 (1984).
[6]P. A. Bennett and J. E. Rowe, Bull. Am. Phys. Soc. **28**, 861 (1983).
[7]K. Takayanagi, Y. Tanishiro, M. Takahashi, and S. Takahashi, J. Vac. Sci. Technol. A **3**, 1502 (1985); K. Takayanagi, Y. Tanishiro, S. Takahashi, and M. Takahashi, Surf. Sci. **164**, 367 (1985).
[8]M. Aono, R. Souda, C. Oshima, and Y. Ishizawa, Phys. Rev. Lett. **51**, 801 (1983).
[9]L. C. Snyder, Surf. Sci. **140**, 101 (1984).
[10]G. Binnig, H. Rohrer, C. Gerber, and E. Weibel, Phys. Rev. Lett. **50**, 120 (1983).
[11]S. Ino, H. Daimon, and T. Hanada, J. Phys. Soc. Jpn. **53**, 1911 (1984).
[12]J. J. Lander and J. Morrison, Surf. Sci. **2**, 553 (1964).
[13]John E. Northrup, Phys. Rev. Lett. **53**, 683 (1984).
[14]G. V. Hansson, R. Z. Bachrach, and R. S. Bauer, J. Vac. Sci. Technol. **18**, 550 (1981).
[15]T. Kinoshita, S. Kono, and T. Sagawa, Phys. Rev. B **32**, 2714 (1985).
[16]J. M. Nicholls, B. Reihl, and John E. Northrup, Phys. Rev. B **35**, 4137 (1987).
[17]For example, K. Saiki, I. Rittaporn, and S. Tanaka, Jpn. J. Appl. Phys. **26**, 45 (1987).
[18]S. Ino, Jpn. J. Appl. Phys. **16**, 891 (1977).
[19]G. Molière, Z. Naturforsch. Teil A: **2**, 133 (1947).
[20]J. M. Hansteen, O. M. Johnsen, and L. Kocbach, At. Data Nucl. Data Tables **15**, 305 (1975).
[21]B. W. Batterman and D. R. Chipman, Phys. Rev. **127**, 690 (1962).
[22]M. Schuster and C. Varelas, Surf. Sci. **157**, 74 (1985).
[23]R. M. Tromp and E. J. Van Loenen, Surf. Sci. **155**, 441 (1985).
[24]T. Yamaguchi, Phys. Rev. B **32**, 2356 (1985).
[25]Guo-Xin Qian and D. J. Chadi, Phys. Rev. B **35**, 1288 (1987).
[26]M. K. Kelly, G. Margaritondo, J. Anderson, D. J. Frankel, and G. J. Lapeyre, J. Vac. Sci. Technol. A **3**, 1481 (1985).
[27]M. K. Kelly, G. Margaritondo, J. Anderson, D. J. Frankel, and G. J. Lapeyre, J. Vac. Sci. Technol. A **4**, 1396 (1986).